



## Re-entry Analyses of Space Debris with Surface Oxidation, Ablation, and By-products Generation

Seong-Hyeon Park<sup>1</sup>, Javier Navarro Laboulais<sup>2</sup>, Pénélope Leyland<sup>3</sup>, Stefano Mischler<sup>4</sup>

### Abstract

The thermal degradation of space debris materials generate chemical by-products which may potentially contribute to atmosphere pollution and trigger adverse chemical reactions for instance for the ozone layer. Predicting the degree of degradation of space debris is therefore of great concern for space agencies such as ESA and NASA in order to mitigate population risks and environmental concerns. With the great concern, the analysis of the re-entry space debris and the estimation of the on-ground risk are becoming important topics in space science. In this paper, analysis of post shock relaxation data and by-products generation has been conducted. The results have shown that there are large differences in between equilibrium post shock assumptions and non-equilibrium assumptions at high altitudes. The non-equilibrium effects are strong at high altitudes, and consequently the equilibrium flow underestimates the flow temperatures as well as dissociated atoms, resulting in a difference in by-products generation, implying the importance of considering the non-equilibrium flow effects on the re-entry analysis.

**Keywords:** space debris, non-equilibrium, by-products, post-shock

### Nomenclature

#### Latin

$e$  – internal energy, [J/kg]  
 $E$  – total energy, [J/kg]  
 $G$  – total Gibbs free energy, [J]  
 $Kn$  – Knudsen number, [-]  
 $n$  – mole number, [mol]  
 $N$  – number of species, [-]  
 $p$  – pressure, [Pa]  
 $q$  – heat flux, [W/m<sup>2</sup>]  
 $R$  – gas constant, [J/K-mol]  
 $t$  – time, [s]  
 $T$  – temperature, [K]  
 $u$  – velocity, [m/s]

#### Greek

$\mu_i$  – chemical potential of component  $i$ , [J/mol]  
 $\dot{\Omega}_{EC}$  – electron-chemistry energy exchange source term, [W/m<sup>3</sup>]

$\dot{\Omega}_{ET}$  – electron-translation energy exchange source term, [W/m<sup>3</sup>]  
 $\dot{\Omega}_{VC}$  – vibration-chemistry energy exchange source term, [W/m<sup>3</sup>]  
 $\dot{\Omega}_{VT}$  – vibration-translation energy exchange source term, [W/m<sup>3</sup>]  
 $\dot{\omega}$  – mass production source term, [kg/m<sup>3</sup>-s]  
 $\rho$  – density, [kg/m<sup>3</sup>]  
**Subscripts**  
 $c$  – condensed species  
 $e$  – free-electrons  
 $g$  – gas species  
 $i$  – component  $i$   
 $j$  – component  $j$   
 $rad$  – radiation  
 $s$  – chemical species  
 $ve$  – vibration-electron-electronic thermal energy mode

<sup>1</sup>Ecole Polytechnique Fédérale de Lausanne EPFL, Tribology and Interface Chemistry Group (SCI-STI-SM), Station 12, Lausanne, CH-1015, Switzerland/Agency for Defense Development, Daejeon, South Korea, shpark2306@gmail.com

<sup>2</sup>Chemical and Nuclear Engineering Department Universitat Politècnica de València UPV, Valencia, Spain, jnavarla@iqn.upv.es

<sup>3</sup>Ecole Polytechnique Fédérale de Lausanne EPFL, Tribology and Interface Chemistry Group (SCI-STI-SM), Station 12, Lausanne, CH-1015, Switzerland, penelope.leyland@epfl.ch

<sup>4</sup>Ecole Polytechnique Fédérale de Lausanne EPFL, Tribology and Interface Chemistry Group (SCI-STI-SM), Station 12, Lausanne, CH-1015, Switzerland, stefano.mischler@epfl.ch

## 1. Introduction

In the Low Earth Orbit (LEO), there is a large amount of existing space debris which have high kinetic energy and they are a serious threat to orbiting objects such as satellites and space stations [1]. In the eventually that such space objects re-entry either deliberately or unintentionally (end of orbital lifetime and uncontrolled) the Earth's atmosphere, a majority of the internal components are completely burned up when impacting the atmosphere. However, the surviving objects could cause injure the human population or damage properties on the ground. Moreover, the thermal degradation of the satellite materials generate chemical by-products that may potentially contribute to atmosphere pollution and trigger adverse chemical reactions for instance for the ozone layer. Predicting the degree of degradation of space debris is therefore of great concern for space agencies such as ESA and NASA in order to mitigate population risks and environmental concerns [2].

With the great concern, the analysis of the re-entry space debris and the estimation of the on-ground risk are becoming important topics in space science. The representative space agencies including ESA and NASA have systematically categorized and conducted these researches. The re-entry break-up, ablation, and analysis tools started to be devised firstly as the most important aspects of the re-entry analysis. To date, the re-entry tools [3-8] such as DEBRISK, ORSAT, SCARAB, and DRAMA/SESAM have been developed to estimate the ground footprints of the eventual falling debris and mitigate these risks, and where both uncontrolled and controlled (deliberate de-orbiting along specific trajectories) situations are pin-pointed. However, there are a lot of uncertainties and much effort is required to have a reasonable reliability in re-entry analysis. In this respect, re-entry analysis, surface oxidation, and chemical by-products generation with ground risk assessment for space debris are challenging topics [2]. Re-entry problems are quite complex and the uncertainties have not been fully understood in the existing tools. Particularly, the effect of the non-equilibrium flow to the re-entry analysis should be noted because it is strongly related to the survivability and thermal break-up [2]. It is known that most of the aforementioned re-entry tools calculate the heat flux assuming an equilibrium flow with fully catalytic wall condition [3,9-11]. But, the equilibrium flow may underestimate the flow temperature as well as dissociated atoms in a shock layer [2]. Across the shock wave, most of the freestream kinetic energy is rapidly transformed into translational energy as they collide with the more dense shock-layer gas. At the same time, most of the molecules are dissociated and recombined due to the high kinetic energy. Inter-particle collisions then excite the rotational, vibrational, ionization, and electronic modes of the molecules, and translational energy begins to relax. Depending on the shock stand-off distance of considered model, the flow may remain in non-equilibrium or reaches equilibrium state. Previous studies have pointed out that the non-equilibrium effects were prominent for the small size object (the time available is far too short compared to relaxation time to reach thermodynamic equilibrium) and/or high altitudes [2,9]. Therefore, the non-equilibrium flow needs to be considered for re-entry analysis.

In this paper, thermo-chemical analysis of re-entering satellite and other space debris material ablation, degradation and the associated by-products released at the surface are combined with a re-entry analysis tool described in [2,9-11]. The developed re-entry tool which is included in an integrated system for the orbit, orbital lifetime, and re-entry survivability estimation modules [1] has been extensively validated with literature. The effects of heating induced by chemical reactions associated to thermal degradation of the underlying materials of the debris have been partially studied for the concerns of the space object material combustion driven by-products in a recent project conducted with ESA, with the final goal of evaluating the environmental impact caused by reentering objects. Particular attention is focused on the effect of non-equilibrium flow at high altitudes. By-products released at the surface are also considered to deeply understand the interaction with the near wall gas condition in-between the boundary layer and the surface of the object, and the effect of the chemical reactions on the net heat flux at the surface.

## 2. Re-entry analysis

In this paper, the object-oriented re-entry analysis tool has been used to estimate the trajectory and survivability. The main feature of this type of tool is the fast simulation that enables users to do extensive parametric and statistical analyses using simple-shaped objects [2]. It is basically composed

of six modules such as trajectory, atmosphere, aerodynamics, aerothermodynamics, thermal analysis, and ablation modules. These modules interact with each other to simulate re-entry analysis. The re-entry tool was first developed in a previous study [9], and it has been improved continuously [1,2] (the re-entry analysis tool is called 'ATD Trajectory Tool (ATD TT)'). Fig. 1 shows the schematic diagram of tool. The trajectory module which can be mathematically described by Newton's equation of motion simulates a three degree-of-freedom trajectory by assuming an object as a mass point. Gravity and aerodynamic forces are considered. In the atmosphere module, the 1976 U.S. Standard Atmosphere Model is used. This module produces the atmospheric temperature, density, and pressure according to the altitude. Aside from this, several atmosphere models such as the NRLMSISE00 can be applied to this module. The aerodynamic module calculates aerodynamic coefficients. The Earth atmosphere can be divided into three flow regimes such as free molecular, transition, and continuum regimes depending on the Knudsen number (Kn). The aerodynamic coefficients can be obtained in accordance with the three regimes. The aerothermodynamics module evaluates heat flux on the surface. The net heat flux is composed of aerodynamic heating, oxidation, and re-radiation. While the aerodynamic heating and oxidation increase heat flux, the re-radiation decreases it. The thermal analysis module can compute surface and inner temperatures of an object by interacting with the aerothermodynamic module. The evaluated heat flux and surface temperature are updated based on the interaction. A nodal thermal math model is used and the innermost node is assumed to be adiabatic. The ablation module determines whether the outer layer of an object is removed or not. If the heat flux from the aerothermodynamics module exceeds the heat of ablation for the outer layer of the object, the layer is assumed to be eliminated [2,9].

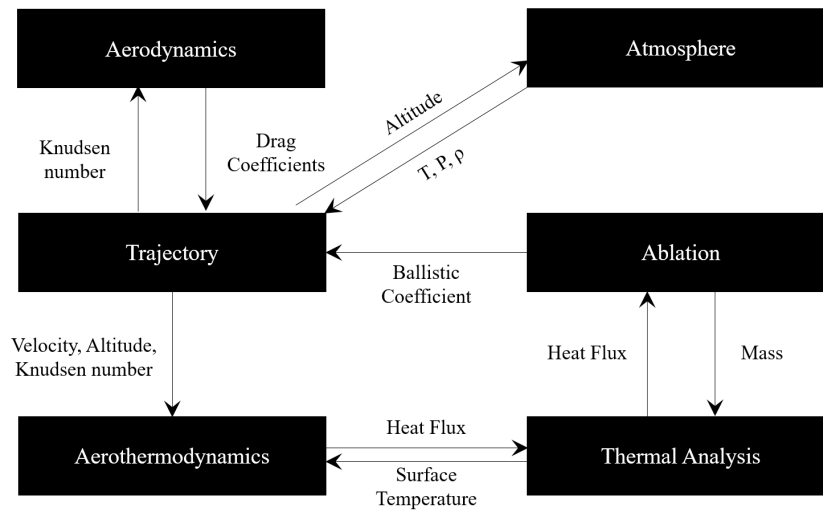


Fig 1. Logic schema of the re-entry tool (ATD TT) [1]

### 3. Post shock relaxation in hypersonic flows

Based on the Poshax3 which is a developed code by University of Queensland, the post shock conditions were numerically calculated [12,13]. The code is an extension of the Post-SHock relAXation solver (Poshax) code originally developed by Gollan to two- and three-temperature gases with fully coupled governing equations [2]. It solves a one-dimensional flow behind a strong shock wave by assuming inviscid flow. Chemical reactions, radiative cooling and thermal energy exchange can be considered as source terms. From the full Navier-Stokes equations, the post shock relaxation equations can be derived. The equations for a two temperature gas can be expressed as follows [2],

$$\frac{\partial \rho_s}{\partial t} + \frac{\partial}{\partial x}(\rho_s u) = \dot{\omega}_s \quad (1)$$

$$\frac{\partial \rho u}{\partial t} + \frac{\partial}{\partial x}(\rho u^2 + p) = 0 \quad (2)$$

$$\frac{\partial \rho E}{\partial t} + \frac{\partial}{\partial x}(u(\rho E + p)) = -\frac{\partial q_{rad}}{\partial x} \quad (3)$$

$$\frac{\partial \rho e_{ve}}{\partial t} + \frac{\partial}{\partial x}(u(\rho e_{ve} + p_e)) = -\frac{\partial q_{rad}}{\partial x} + \dot{\Omega}_{VT} + \dot{\Omega}_{ET} + \dot{\Omega}_{VC} + \dot{\Omega}_{EC} \quad (4)$$

where the upper dot denotes differentiation with respect to time. Eqs. (1)-(4) are derived based on conservation equations for momentum, species mass, and energy. The vibration and electron-electronic energy equations for a three temperature model are expressed as [2,13],

$$\frac{\partial}{\partial x}(ue_v) = \dot{\Omega}_{VT} + \dot{\Omega}_{VE} + \dot{\Omega}_{VC} \quad (5)$$

$$\frac{\partial}{\partial x} + \frac{\partial}{\partial x}(ue_e + p_e) = -\frac{\partial q_{rad}}{\partial x} + \dot{\Omega}_{ET} + \dot{\Omega}_{EV} + \dot{\Omega}_{EC} \quad (6)$$

In this study, 11 species air model was considered and the spatial step ( $\Delta x$ ) was set to  $10^{-5}$  m. The viscosity for gas-mixture was obtained by the Gupta-Yos's mixture rule [14]. The chemical-kinetic and vibration-transition energy exchange model by Park [15] was used with the translation-electron energy exchange model by Gnoffo [16].

#### 4. By-products generation

The ablation phenomenon during re-entry causes the formation of chemical by-products. The generated by-products are different depending on the original composition of the object and atmospheric air. At hypersonic flow, the aerothermodynamic heating increases the surface temperature and leads to ablation of its complex components. In the boundary layer edge, the temperature and pressure determine the thermodynamic chemically stable by-products. The method used in this study is based on the Gibbs Energy Minimisation (GEM) where chemical compositions are determined for a closed system at given pressure and temperature, minimising the Gibbs free energy [2,17,18]. Based on the above-mentioned re-entry analysis tool, the ablated mass, and pressure and temperature of post shock conditions can be obtained according to re-entry trajectory. Atmospheric composition of  $N_2 = 79\%$  and  $O_2 = 21\%$  is assumed to be constant below 100 km. From the given conditions, the emitted by-products composition can be determined by GEM. The relationship between the minimisation of the Gibbs free energy and atomic composition balance is expressed as follows [2],

$$\min G(P, T, n) = \sum_N n_i \cdot \mu_i(P, T, n) \quad (7)$$

$$An = b, \quad \text{with } n \geq 0 \quad (8)$$

where  $\mathbf{A}$  is the atomic matrix relating the chemical species with atomic composition and  $\mathbf{b}$  is the element abundance vector [2]. The chemical potential for ideal system can be expressed with regard to molar composition. But, the chemical potential for the real system consists of gas and condensed phases. Therefore, Eq. (7) can be splitted as follows [2],

$$\min G(P, T, n) = \sum_{N_c} n_i \cdot \mu_i(T, N_c) + \sum_{N_g} n_j \cdot \mu_j(P, T, N_g) \quad (9)$$

The chemical potential for gas and and condensed species can be written as,

$$\mu_i(T, N_c) = \mu_i^\circ(T) \quad (10)$$

$$\mu_j(P, T, N_g) = \mu_j^\circ(T) + RT \ln\left(\frac{n_j}{\sum_{N_g} n_j}\right) + RT \ln\left(\frac{P}{P^\circ}\right) \quad (11)$$

where  $\mu_i^\circ(T)$  and  $\mu_j^\circ(T)$  are the standard chemical potentials or conversely, the chemical potential in the standard state, and  $P^\circ$  is the pressure of reference at ground level [2]. The general procedure for the calculation of the by-products generation along the re-entry trajectory can be expressed in the following order: (1) compound identification in the whole database after the enumeration of the chemical elements initially present in the system, (2) atomic composition balance considering the initial chemicals and the air excess considered for the computation, (3) minimisation of the Gibbs free energy, (4) data post-processing for the evaluation of by-products emission profiles along the trajectory. The detailed explanations can be found in Ref. [2]. The re-entry ATDDT can provide pressure, temperature, and ablated mass gradient according to the trajectory with the by-product model estimation. Based on the minimisation of the Gibbs free energy, the chemical compositions are determined and by-product generations are calculated from data post-processing with the ablated mass gradient.

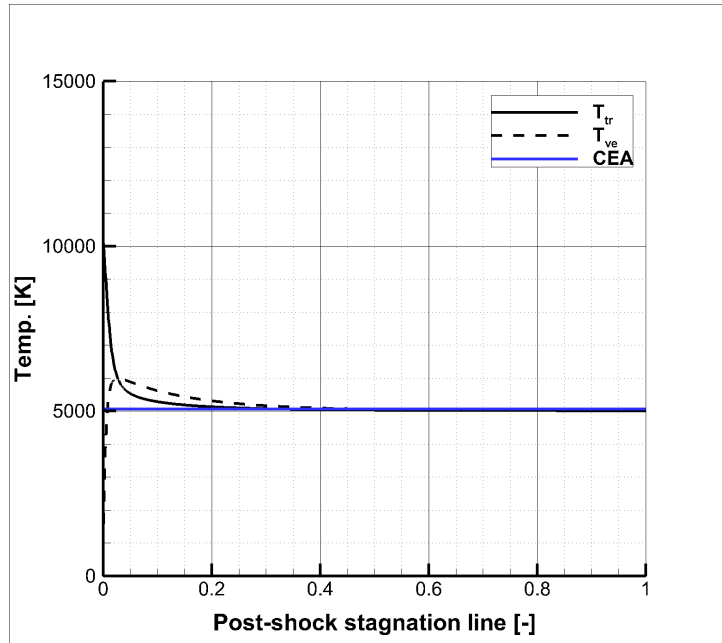
## 5. Results and discussion

To investigate the effect of non-equilibrium flow on the re-entry analysis, post shock conditions are estimated along the re-entry trajectory. In the calculations, the Park's two temperature model was considered. Particular attention is given to two different trajectory points representing low and high altitudes, respectively. The first point represents an altitude of 40 km where the freestream velocity is about 4500 m/s and atmospheric density, temperature, and pressure are 0.004 kg/m<sup>3</sup>, 250 K, and 290 Pa, respectively. The second point represents an altitude of 80 km where the freestream velocity, density, temperature, and pressure are 7310 m/s, 0.000019 kg/m<sup>3</sup>, 200 K, and 1.06 Pa, respectively.

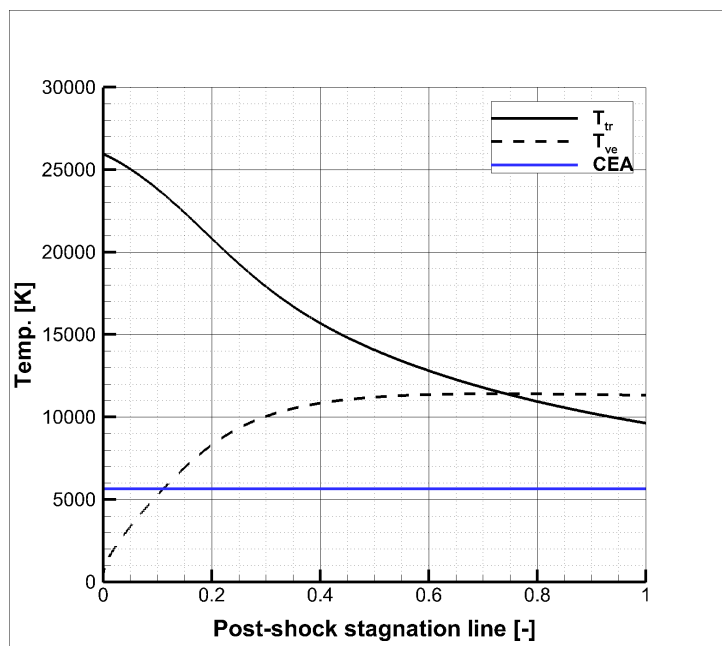
Figs. 2 and 3 show the post shock temperature profiles. In the figures,  $T_{tr}$  and  $T_{ve}$  represent translational-rotational temperature and vibrational-electronic temperature, respectively. The calculated equilibrium temperature from the Chemical Equilibrium Compositions and Applications (CEA) program is also considered for the comparison. Across the shock wave, most of the freestream kinetic energy is rapidly transformed into translational energy as they collide with the more dense shock-layer gas. Most of the molecules are dissociated and recombined due to the high kinetic energy. Inter-particle collisions then excite the rotational, vibrational, ionization, and electronic modes of the molecules, and translational energy begins to relax. Looking at Fig. 2, the translational temperature rapidly increases after the shock wave and decreases further downstream as the molecules are dissociated, and the vibrational-electronic temperature also increases and decreases following the translational temperature. Before the flow reaches the wall of the object, the temperatures get to the local equilibrium state. It also can be noted that the two temperatures are in good agreement with the equilibrium flow temperature by the CEA. However, in Fig. 3, the two temperatures are not corresponding to the equilibrium state at an altitude of 80 km. Compared to the calculated equilibrium temperature by CEA, the non-equilibrium temperatures are higher which means that the equilibrium flow underestimates the flow temperature. The results have shown that the non-equilibrium effects are strong at such relatively high altitudes. For further comparison, the post shock mass fraction profiles are shown in Figs. 4 and 5. The two temperature 11 species air model ( $N_2$ ,  $O_2$ , N, O, NO,  $N_2^+$ ,  $O_2^+$ ,  $N^+$ ,  $O^+$ ,  $NO^+$ ,  $e^-$ ) was considered in the calculations. Looking at Fig. 4, the mass fraction of species is presented at an altitude of 40 km. Behind the shock wave, the mass fraction remains constant as the temperatures reach the equilibrium state. While the mass fraction of  $N_2$  is nearly constant, that of  $O_2$  is partially dissociated considering the translational temperature. However, in Fig. 5, the mass fractions of  $N_2$  and  $O_2$  continue to decrease as the flow approaches the wall of the object at an altitude of 80 km. Consequently, the mass fractions of the other species (N, O, NO,  $N_2^+$ ,  $O_2^+$ ,  $N^+$ ,  $O^+$ ,  $NO^+$ ,  $e^-$ ) resulting from  $N_2$  and  $O_2$  are higher than those of an altitude of 40 km. It can be noted that the non-equilibrium effects are strong at high altitudes, and consequently the equilibrium flow underestimates the dissociated atoms.

Fig. 6 shows the by-products emission profiles for the aluminium material. The coupling of the ATDDT tool and the GEM tool allows a detailed by-product analysis along the re-entry trajectory. The calculations in the ATDDT tool were performed using equilibrium air chemistry post shock assumptions (EQ) and non-equilibrium ones (NEQ). In the figure, the object is consumed starting from an altitude of 80 km in the

non-equilibrium case (NEQ), whereas the ablation only starts around 60 km for the equilibrium chemistry case (EQ). The produced species are  $N_2$ ,  $O_2$ ,  $NO$ ,  $NO_2$ ,  $Al(cr)$ ,  $Al_2O_3(a)$ , and  $O_2^*$ . Among them,  $N_2$ ,  $O_2$ , and  $Al_2O_3(a)$  are evident. The importance here is the production of oxides at higher altitudes, the particles of these by-products remain for more time within the atmosphere in the NEQ than in the EQ, which will have a long-term impact on atmospheric chemistry. The temperatures and dissociated atoms of NEQ are higher than those of EQ which means that more by-products emissions are expected causing the atmospheric environmental impact from re-entry.



**Fig 2.** Post shock temperature profiles at 40 km



**Fig 3.** Post shock temperature profiles at 80 km

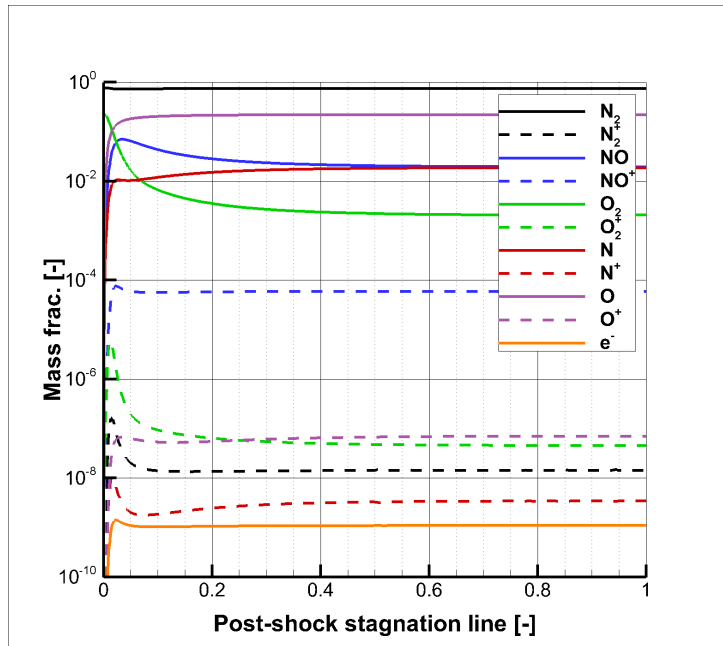


**Fig 4.** Post shock mass fraction profiles at 40 km

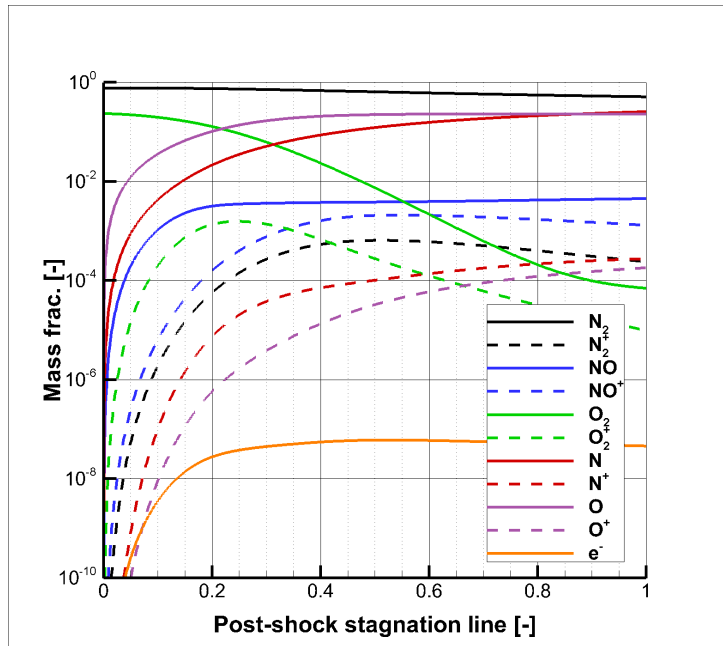


**Fig 5.** Post shock mass fraction profiles at 80 km

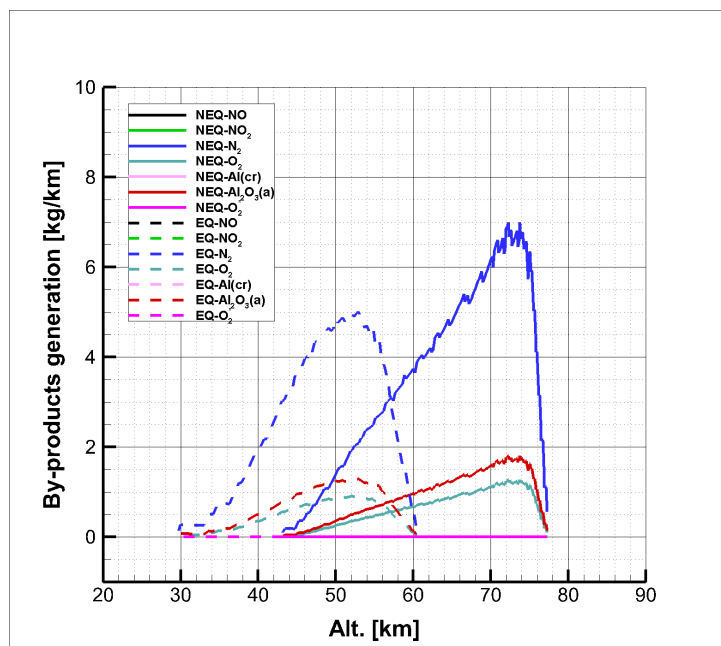


**Fig 6.** By-products emissions for aluminium

## 6. Conclusions

Post shock relaxation data and by-products generation have been investigated during re-entry. Based on the Poshax3 which is an extension of the Post-SHock relAXation solver (Poshax) code, post shock conditions were estimated along the re-entry trajectory. In the simulations, the two temperature 11 species air model was considered. Particular attention was given to two different trajectory points representing low and high altitudes. The results have shown that post shock temperatures and mass fractions of species are in good agreement with those of equilibrium flow estimated using the CEA at low altitudes. However, there were large differences in post shock conditions at high altitudes. It can be noted that the non-equilibrium effects are strong at high altitudes, and consequently the equilibrium flow underestimates the flow temperatures as well as dissociated atoms. Furthermore, the by-products emissions were estimated based on the Gibbs Energy Minimisation (GEM). The calculations were performed using equilibrium air chemistry post shock assumptions (EQ) and non-equilibrium ones (NEQ). It was found that by-products remain for more time within the atmosphere in the NEQ than in the EQ, which means that the NEQ has a long-term impact on atmospheric chemistry, implying the importance of considering the non-equilibrium flow effects on the re-entry analysis. The effect of these effects on materials representative of spacecraft components composition will be presented at the conference.

## References

1. Park, S.-H., Kim, H.-D., Park, G.: Orbit, orbital lifetime, and reentry survivability estimation for orbiting objects. *Adv. Space Res.* 62(11), 3012–3032 (2018)
2. Park, S.-H., Laboulais, J. Navarro, Leyland, P., Mischler, S.: Re-entry survival analysis and ground risk assessment of space debris considering by-products generation. *Acta Astronaut.* 179, 604–618 (2021)
3. Lips, T., Fritsche, B.: A comparison of commonly used re-entry analysis tools. *Acta Astronaut.* 57(2-8), 312–323 (2005)
4. Lips, T., Fritsche, B., Koppenwallner, G.: Spacecraft destruction during re-entry - latest results and development of the scarab software system. *Adv. Space Res.* 34(5), 1055–1060 (2004)

5. Fritsche, B., Lips, T., Koppenwallner, G.: Analytical and numerical reentry analysis of simple-shaped objects. *Acta Astronaut.* 60(8-9), 737–751 (2007)
6. Ostrom, C., Sanchez, C.: Orsat modelling and assessment. (03 2018)
7. Fuentes, I.P., Bonetti, D., Letterio, F., de Miguel, G.V., Arnao, G.B., Palomo, P., Parigini, C., Lemmens, S., Lips, T., Kanzler, R.: Upgrade of esa's debris risk assessment and mitigation analysis (drama) tool: spacecraft entry survival analysis module. *Acta Astronaut.* 158, 148-160 (2019)
8. Annaloro, J., Galera, S., Thiebaut, C., Spel, M., Van Hauwaert, P., Grossir, G., Paris, S., Chazot, O., Omaly, P.: Aerothermodynamics modelling of complex shapes in the debris atmospheric reentry tool: methodology and validation. *Acta Astronaut.* 171, 388-402 (2020)
9. Park, S.-H., Park, G.: Reentry trajectory and survivability estimation of small space debris with catalytic recombination. *Adv. Space Res.* 60(5), 893-906 (2017)
10. Park, S.-H., Neeb, D., Plyushchev, G., Leyland, P., Gülhan, A.: A study on heat flux predictions for re-entry flight analysis. *Acta Astronaut.* 187(2-8), 271-280 (2021)
11. Park, S.-H., Mischler, S., Leyland, P.: Re-entry analysis of critical components and materials for design-for-demise techniques. *Adv. Space Res.* 68(1), 1-24 (2021)
12. Gollan, R.J.: The computational modelling of high-temperature gas effects with application to hypersonic flows. Ph.D. Thesis, University of Queensland (2008)
13. Potter, D.F.: Modelling of radiating shock layers for atmospheric entry at earth and mars. Ph.D. Thesis, University of Queensland (2010)
14. Gupta, R.N., Yos, J.M., Thompson, R.A., Lee, K.-P.: A review of reaction rates and thermodynamic and transport properties for an 11-species air model for chemical and thermal nonequilibrium calculations to 30,000 K. Technical Report, NASA-RP-1232 (1990)
15. Park, C.: Review of chemical-kinetic problems of future nasa missions, I: Earth entries. *J. Thermophys. Heat Tran.* 7(3), 385-398 (1993)
16. Gnoffo, P.A., Gupta, R.N., Shinn, J.L.: Conservation equations and physical models for hypersonic air flows in thermal and chemical nonequilibrium. Technical Report, NASA-TP-2867. (1989)
17. Smith, W., Qi, W.: Molecular simulation of chemical reaction equilibrium by computationally efficient free energy minimization. *Acs Central Sci.* 4(9), 1185-1193 (2018)
18. Smith, W.R., Missen, R.W.: Strategies for solving the chemical equilibrium problem and an efficient microcomputer-based algorithm. *Can. J. Chem. Eng.* 66(4), 591-598 (1988)